Radiation forces in the discrete-dipole approximation

A. G. Hoekstra and M. Frijlink

Section Computational Science, University of Amsterdam, Kruislaan 403, 1098 SJ Amsterdam, The Netherlands

L. B. F. M. Waters

Astronomical Institute "Anton Pannekoek," University of Amsterdam, Kruislaan 403, 1098 SJ Amsterdam, The Netherlands, and Astronomical Institute, Katholic University Leuven, Celestijnenlaan 200B, B-3001 Heverlee, Belgium

P. M. A. Sloot

Section Computational Science, University of Amsterdam, Kruislaan 403, 1098 SJ Amsterdam, The Netherlands

Received July 26, 2000; revised manuscript received January 22, 2001; accepted January 29, 2001

The theory of the discrete-dipole approximation (DDA) for light scattering is extended to allow for the calculation of radiation forces on each dipole in the DDA model. Starting with the theory of Draine and Weingartner [Astrophys. J. **470**, 551 (1996)] we derive an expression for the radiation force on each dipole. These expressions are reformulated into discrete convolutions, allowing for an efficient, $O(N \log N)$ evaluation of the forces. The total radiation pressure on the particle is obtained by summation of the individual forces. The theory is tested on spherical particles. The resulting accumulated radiation forces are compared with Mie theory. The accuracy is within the order of a few percent, i.e., comparable with that obtained for extinction cross sections calculated with the DDA. © 2001 Optical Society of America

OCIS codes: 260.2110, 290.0290, 290.5850.

1. INTRODUCTION

Light carries momentum and may therefore exert a force on a particle on which it impinges. The notion of radiation force, that is, the force exerted by an electromagnetic field on matter with which it interacts, is already very old and was originally analyzed by Maxwell. Debye, in 1909, was probably the first to calculate the radiation force on a small particle, in his case on a sphere.[1] By integrating the electromagnetic stress tensor over the surface of the sphere, he demonstrated that

$$C_{\mathrm{pr}} = C_{\mathrm{ext}} - gC_{\mathrm{sca}}, \tag{1}$$

where C_{pr} is the radiation pressure cross section, C_{ext} the extinction cross section, C_{sca} the scattering cross section, and g the asymmetry parameter. This expression holds for any small particle illuminated by a beam of light.[2]

With the introduction of lasers, radiation force became a powerful tool in the laboratory. Ashkin and Dziedzic, in a spectacular experiment, showed for the first time that it is possible to levitate a small micrometer-sized particle with a laser beam.[3,4] Besides small spheres they also levitated nonspherical particles[5] and biological cells.[6] This pioneering work was extended by Steven Chu, who trapped and cooled single molecules and atoms, thus opening up a complete new field in physics (which won him, together with C. Cohen-Tannoudji and W. D. Philips, the Nobel Prize in physics in 1997).[7] It also led to the development of optical tweezers; see, e.g., Refs. 8 and 9. These optical tweezers allow the micromanipulation of small objects and are used specifically in (molecular) biological experiments.[9] The applications range from cell biology (e.g., Ref. 10) to the study of single DNA molecules. For instance, the elasticity of a single DNA molecule can be measured by attaching both ends of a DNA molecule to small spheres and trapping the spheres in optical tweezers.[9,11] Optical levitation and optical tweezers also allow very detailed light-scattering experiments, where a single micrometer-sized particle is held in a trap, thus allowing the measurement of scattered light by a single particle. In this way, scattering of a single evaporating water droplet was measured, experimentally demonstrating very sharp resonances in Mie scattering.[12] Furthermore, the differential scattering cross sections of single spheres (e.g., Ref. 13) and of single biological cells[14] were measured.

The radiation force also plays an important role in astrophysics. For instance, Draine and Weingartner propose that radiation forces may be responsible for super thermal spin-up of small particles, thus allowing their alignment in the galactic magnetic field.[15,16] This alignment of interstellar dust grains then explains the polarization of starlight. Radiation forces play an important role in the dynamics of cometary and asteroidal dust, of dust in the solar dust ring, and of circumstellar dust; see, e.g., Refs. 17–19.

Dust particles play an important role in the evolution of protoplanetary disks that probably surround all newly born stars. In these disks, dust particles from interstellar space collect and coalesce to form larger aggregates.

0740-3232/2001/081944-10$15.00

These eventually can grow into kilometer-sized bodies (cometary nuclei) or even into planets. The interplay between radiation and dust can strongly influence the growth of dust aggregates, since radiation pressure acts differently on dust of different size, shape, and chemical composition. Also, radiation pressure may result in nonradially directed forces on aggregates, which could have important consequences for dust growth.

The total radiation pressure on the dust particles is not the only important effect. It is suspected that in the detailed process of formation of dust particles in a circumstellar disk, i.e., coagulation of small grains into aggregates,[20] radiation forces could play an important role.[21] For studying the importance of radiation forces on the formation of dust particles, knowledge of the total radiation pressure on the particle is therefore not enough. It is also necessary to know the radiation forces acting on *each* constituent grain in the dust particle. This notion motivated us to extend a method for calculating radiation forces in the discrete-dipole approximation (DDA) of light scattering, such that it allows efficient calculation of the forces on each individual dipole of the DDA. That is the main topic of this paper.

Today, many theories for calculating light scattering from small particles exist; see, e.g., Ref. 22 for a recent overview. Our main interest is in radiation forces on the grains that build up highly irregular dust particles. We choose to use the DDA method to calculate scattering from, and radiation forces on, these particles: first, because the DDA has proven to be a suitable method for calculating scattering from aggregates[23–26] and second, because DDA provides a straightforward way to calculate radiation forces, as will be demonstrated below.

Methods for calculating the radiation pressure in the DDA by applying Eq. (1) were given by Draine.[27] Draine and Weingartner[15] and Kimura and Mann[18] incorporated into the DDA the possibility of calculating radiation pressure by integrating the momentum carried by the scattered radiation over the total space angle. Draine and Weingartner were interested in radiative torques, whereas Kimura and Mann looked at radiation forces that are parallel as well as perpendicular to the direction of incident light. These perpendicular forces may arise for particles that have no highly symmetrical shape. Kimura and Mann immediately applied Eq. (1) and calculated gC_{sca} by an integration of the scattered fields as obtained from the DDA calculations. However, by providing a vector character to g and interpreting it as the mean direction of the scattered light, they could also calculate the perpendicular components of the radiation force. In contrast, Draine and Weingartner started with the DDA equations and a general expression for the force on a dipole in an electromagnetic field. Next they derived a formal expression for the force on each dipole in the DDA. They did not further elaborate these formal expressions, but by invoking a straightforward argument they recovered Eq. (1). They subsequently obtained the radiation forces by calculating gC_{sca} by an integration of the scattered fields.

In this paper we take the work of Draine and Weingartner[15] as a starting point and derive expressions for the radiation force on each dipole in the DDA. We test our procedure by calculating the radiation force on a sphere and compare DDA results with exact Mie calculations.

2. THEORY OF RADIATION FORCES IN THE DISCRETE-DIPOLE APPROXIMATION

A. Radiation Force on a Single Dipole in the Discrete-Dipole Approximation

The DDA[28,29] models a particle as an array of N point dipoles at position $\mathbf{r}_i$ with polarizability α_i. The force on a point dipole i in an electromagnetic field is[30]

$$\mathbf{F}_i = \mathrm{Re}(\mathbf{p}_i \cdot \nabla_i)\mathrm{Re}(\mathbf{E}_i) + \frac{1}{c}\mathrm{Re}\left(\frac{\mathrm{d}\mathbf{p}_i}{\mathrm{d}t}\right) \times \mathrm{Re}(\mathbf{B}_i), \quad (2)$$

where $\mathbf{E}_i$ and $\mathbf{B}_i$ are the electric and the magnetic field on dipole i, $\mathbf{p}_i$ is the dipole moment on dipole i, c is the speed of light in vacuum, and t denotes time. For harmonic fields, time averaging of Eq. (2) results in

$$\langle \mathbf{F}_i \rangle = \frac{1}{2}\mathrm{Re}[(\mathbf{p}_i^* \cdot \nabla_i)\mathbf{E}_i + ik\mathbf{p}_i^* \times \mathbf{B}_i], \quad (3)$$

where the asterisk denotes complex conjugation, $k = |\mathbf{k}|$, and $\mathbf{k}$ is the wave vector. We will now derive an expression for $\langle \mathbf{F}_i \rangle$ in the context of the DDA model.

Following Draine and Weingartner,[15] the time-averaged force on a dipole is split into two components, one due to the incident field and the other due to the fields radiated by all other dipoles:

$$\langle \mathbf{F}_i \rangle = \langle \mathbf{F}_{\mathrm{inc},i} \rangle + \langle \mathbf{F}_{\mathrm{sca},i} \rangle. \quad (4)$$

Note that the averaged total radiation force on the particle, modeled by the collection of N dipoles, can be expressed as

$$\langle \mathbf{F}_{\mathrm{rad}} \rangle = \langle \mathbf{F}_{\mathrm{inc}} \rangle + \langle \mathbf{F}_{\mathrm{sca}} \rangle = \sum_{i=1}^{N} \langle \mathbf{F}_{\mathrm{inc},i} \rangle + \sum_{i=1}^{N} \langle \mathbf{F}_{\mathrm{sca},i} \rangle. \quad (5)$$

Draine and Weingartner[15] show that

$$\langle \mathbf{F}_{\mathrm{inc},i} \rangle = \frac{1}{2}\mathrm{Re}\{(\mathbf{p}_{i,0}^* \cdot \nabla_i)[\mathbf{E}_{\mathrm{inc},0}\exp(i\mathbf{k} \cdot \mathbf{r}_i)] + ik\mathbf{p}_{i,0}^* \times [\hat{\mathbf{k}} \times \mathbf{E}_{\mathrm{inc},0}\exp(i\mathbf{k} \cdot \mathbf{r}_i)]\}, \quad (6)$$

$$\langle \mathbf{F}_{\mathrm{sca},i} \rangle = \sum_{j \neq i} \frac{1}{2}\mathrm{Re}[(\mathbf{p}_{i,0}^* \cdot \nabla_i)\mathbf{E}_{ij} + ik\mathbf{p}_{i,0}^* \times \mathbf{B}_{ij}], \quad (7)$$

where $\mathbf{E}_{\mathrm{inc},0}$ is the amplitude of the incoming plane wave, $\mathbf{p}_{i,0}$ is the amplitude of the dipole moment on dipole i, and

$$\mathbf{E}_{ij} = \frac{\exp(ikr_{ij})}{r_{ij}^3}\left\{k^2\mathbf{r}_{ij} \times (\mathbf{p}_{j,0} \times \mathbf{r}_{ij}) + \frac{(1 - ikr_{ij})}{r_{ij}^2}[3\mathbf{r}_{ij}(\mathbf{r}_{ij} \cdot \mathbf{p}_{j,0}) - r_{ij}^2\mathbf{p}_{j,0}]\right\}, \quad (8)$$

$$\mathbf{B}_{ij} = k^2\frac{\exp(ikr_{ij})}{r_{ij}^2}(\mathbf{r}_{ij} \times \mathbf{p}_{j,0})\left(1 - \frac{1}{ikr_{ij}}\right), \quad (9)$$

with $r_{ij} = |\mathbf{r}_{ij}|$, $\mathbf{r}_{ij} = \mathbf{r}_i - \mathbf{r}_j$. Evaluating Eq. (6) results in

$$\langle \mathbf{F}_{\mathrm{inc},i} \rangle = \frac{1}{2} \mathrm{Re}[i\mathbf{k}(\mathbf{p}_{i,0}^* \cdot \mathbf{E}_{\mathrm{inc},0}) \exp(i\mathbf{k} \cdot \mathbf{r}_i)]. \quad (10)$$

When the expression for the extinction coefficient in the DDA as obtained from the optical theorem is applied,[27] the final expression for $\langle \mathbf{F}_{\mathrm{inc}} \rangle$ becomes

$$\langle \mathbf{F}_{\mathrm{inc}} \rangle = \frac{1}{8\pi} C_{\mathrm{ext}} |\mathbf{E}_{\mathrm{inc},0}|^2 \hat{\mathbf{k}}. \quad (11)$$

$\langle \mathbf{F}_{\mathrm{inc}} \rangle$ can be interpreted as the average rate by which momentum is removed from the incident beam. This force is in the direction of the incident beam. The next step is to calculate $\langle \mathbf{F}_{\mathrm{sca},i} \rangle$ from Eq. (7). This was not done, however, by Draine and Weingartner, because it would lead to summations involving $N(N-1)$ terms, which could be computationally prohibitive.[15] They did suggest, however, that this operation count could be reduced to $O(N \log N)$ by using fast Fourier-transform techniques. Below we will explicitly calculate $\langle \mathbf{F}_{\mathrm{sca},i} \rangle$ and demonstrate how the operation count can indeed be reduced, but first we will show how Draine and Weingartner proceeded.

By invoking momentum conservation we can easily show that the net rate of momentum transported to infinity by the scattered field, denoted by $\langle \mathbf{F}_{\mathrm{out}} \rangle$, must be equal to $-\langle \mathbf{F}_{\mathrm{sca}} \rangle$. Draine and Weingartner[15] show that

$$\langle \mathbf{F}_{\mathrm{out}} \rangle = \frac{k^4}{8\pi} \int \mathrm{d}\Omega \hat{\mathbf{n}} \left| \sum_{i=1}^{N} [\mathbf{p}_{i,0} - \hat{\mathbf{n}}(\hat{\mathbf{n}} \cdot \mathbf{p}_{i,0})] \times \exp(-ik\hat{\mathbf{n}} \cdot \mathbf{r}_i) \right|^2, \quad (12)$$

with $\hat{\mathbf{n}}$ the direction vector on the unit sphere. Compare Eq. (12) with the expression for the asymmetry parameter $\mathbf{g}$, in vector form, as defined by Kimura and Mann,[18]

$$g_j = \frac{k^4}{C_{\mathrm{sca}} |\mathbf{E}_{\mathrm{inc},0}|^2} \int \mathrm{d}\Omega \hat{\mathbf{n}} \cdot \hat{\mathbf{e}}_j \times \left| \sum_{i=1}^{N} [\mathbf{p}_{i,0} - \hat{\mathbf{n}}(\hat{\mathbf{n}} \cdot \mathbf{p}_{i,0})] \exp(-ik\hat{\mathbf{n}} \cdot \mathbf{r}_i) \right|^2, \quad (13)$$

where $\mathbf{g} = g_1\hat{\mathbf{e}}_1 + g_2\hat{\mathbf{e}}_2 + g_3\hat{\mathbf{e}}_3$ and $(\hat{\mathbf{e}}_1, \hat{\mathbf{e}}_2, \hat{\mathbf{e}}_3)$ form Cartesian basis vectors with $\hat{\mathbf{e}}_1 = \hat{\mathbf{k}}$, i.e., in the direction of the incident wave. This results in

$$\langle \mathbf{F}_{\mathrm{out}} \rangle = \frac{1}{8\pi} C_{\mathrm{sca}} |\mathbf{E}_{\mathrm{inc},0}|^2 \mathbf{g}. \quad (14)$$

By defining the radiation pressure cross-section vector through

$$\langle \mathbf{F}_{\mathrm{rad}} \rangle = \frac{1}{8\pi} |\mathbf{E}_{\mathrm{inc},0}|^2 \mathbf{C}_{\mathrm{pr}} \quad (15)$$

and combining Eqs. (5), (11), (14), and (15), we find that

$$\mathbf{C}_{\mathrm{pr}} = C_{\mathrm{ext}}\hat{\mathbf{k}} - C_{\mathrm{sca}}\mathbf{g}. \quad (16)$$

In the direction of the incident beam, Eq. (16) reduces to Eq. (1). Both Kimura and Mann[18] and Draine and Weingartner[15] numerically evaluated the integral in Eq. (12) or Eq. (13) to arrive at the total radiation force on the particle. Note that evaluation of these integrals requires $O(N_s N)$ operations, with N_s the number of scattering directions required for accurate evaluation of the integrals.

We will now demonstrate how to calculate $\langle \mathbf{F}_{\mathrm{sca},i} \rangle$ directly from the dipole polarizabilities. Furthermore, we will demonstrate the correspondence between this direct method and the integration in Eqs. (12) and (13).

First, it is convenient to reformulate Eq. (8) into

$$\mathbf{E}_{ij} = \exp(ikr_{ij}) \left[\left(\frac{k^2}{r_{ij}} + \frac{ik}{r_{ij}^2} - \frac{1}{r_{ij}^3} \right) \mathbf{p}_{j,0} + \left(-\frac{k^2}{r_{ij}} - \frac{3ik}{r_{ij}^2} + \frac{3}{r_{ij}^3} \right) \hat{\mathbf{n}}_{ij} (\hat{\mathbf{n}}_{ij} \cdot \mathbf{p}_{j,0}) \right], \quad (17)$$

where $\hat{\mathbf{n}}_{ij} = \mathbf{r}_{ij}/r_{ij}$. To calculate $\langle \mathbf{F}_{\mathrm{sca},i} \rangle$ from Eq. (7) we need to evaluate $(\mathbf{p}_i^* \cdot \nabla_i)\mathbf{E}_{ij}$. From Eq. (17) it is clear that this boils down to four nontrivial differentiations. These calculations are performed in Appendix A. The magnetic term in Eq. (7) is straightforward:

$$\begin{aligned} ik\mathbf{p}_{i,0}^* \times \mathbf{B}_{ij} &= ik^3 \frac{\exp(ikr_{ij})}{r_{ij}} \mathbf{p}_{i,0}^* \times (\hat{\mathbf{n}}_{ij} \times \mathbf{p}_{j,0}) \left(1 - \frac{1}{ikr_{ij}} \right) \\ &= \left(\frac{ik^3}{r_{ij}} - \frac{k^2}{r_{ij}^2} \right) [(\mathbf{p}_{i,0}^* \cdot \mathbf{p}_{j,0})\hat{\mathbf{n}}_{ij} - (\mathbf{p}_{i,0}^* \cdot \hat{\mathbf{n}}_{ij})\mathbf{p}_{j,0}] \exp(ikr_{ij}). \end{aligned} \quad (18)$$

Combining all terms results in

$$\langle \mathbf{F}_{\mathrm{sca},i} \rangle = \sum_{j \neq i} \frac{1}{2} \mathrm{Re}(\mathbf{F}_{ij}), \quad (19)$$

with

$$\begin{aligned} \mathbf{F}_{ij} = \exp(ikr_{ij}) \Bigg\{ & [(\mathbf{p}_{i,0}^* \cdot \mathbf{p}_{j,0})\hat{\mathbf{n}}_{ij} + \mathbf{p}_{i,0}^* (\hat{\mathbf{n}}_{ij} \cdot \mathbf{p}_{j,0}) \\ & + (\mathbf{p}_{i,0}^* \cdot \hat{\mathbf{n}}_{ij})\mathbf{p}_{j,0} - 5(\mathbf{p}_{i,0}^* \cdot \hat{\mathbf{n}}_{ij})\hat{\mathbf{n}}_{ij}(\hat{\mathbf{n}}_{ij} \cdot \mathbf{p}_{j,0})] \\ & \times \left(-\frac{k^2}{r_{ij}^2} - \frac{3ik}{r_{ij}^3} + \frac{3}{r_{ij}^4} \right) + [(\mathbf{p}_{i,0}^* \cdot \mathbf{p}_{j,0})\hat{\mathbf{n}}_{ij} \\ & - (\mathbf{p}_{i,0}^* \cdot \hat{\mathbf{n}}_{ij})\hat{\mathbf{n}}_{ij}(\hat{\mathbf{n}}_{ij} \cdot \mathbf{p}_{j,0})] \left(\frac{ik^3}{r_{ij}} - \frac{k^2}{r_{ij}^2} \right) \Bigg\}. \end{aligned} \quad (20)$$

Equations (19) and (20) provide the force on each dipole that is due to the field radiated from all other dipoles. Taking Eqs. (19) and (20) together with Eq. (10), we obtain the total radiation force $\langle \mathbf{F}_i \rangle$ on each dipole. In Appendix B we show, by analytically solving the integral in Eq. (12), that the resulting expressions for $\langle \mathbf{F}_{\mathrm{sca}} \rangle$ are indeed equal to $-\langle \mathbf{F}_{\mathrm{out}} \rangle$. We will continue to show how the calculation of the forces can be formulated as a discrete convolution, thus allowing an $O(N \log N)$ calculation of the forces.

B. $O(N \log N)$ Algorithm for the Forces

The computational burden in evaluating the radiation force directly from the dipole moments comes from the summation in Eq. (19) in combination with the summation in Eq. (5). This leads to an $O(N^2)$ operation count, which is prohibitive if N becomes large. Therefore, if one wants to calculate the total radiation force on a particle, it is obviously more efficient to numerically evaluate the integrals of Eqs. (12) and (13). However, if one wants to calculate the forces on each single dipole (as in our intended application of radiation forces on the constituent grains of an aggregate dust particle), we must use Eq. (19) for all N dipoles.

Fortunately, just as the matrix vector products in the conjugate-gradient iteration that is used to solve the DDA field equations are nothing but discrete convolutions,[31] the expression for $\langle \mathbf{F}_{\mathrm{sca}} \rangle$ can be written as a discrete convolution. With the dipoles located on a rectangular grid, fast Fourier transforms can be used to reduce the operation count to $O(N \log N)$. This is obviously a very important computational improvement for the calculation of the radiation forces on each single dipole. Furthermore, if the number N_s of evaluation points of the numerical integration of Eqs. (12) and (13) is large, the $O(N \log N)$ operation count of the direct method is also a computational improvement over the integration method.

A close look at Eq. (20) already makes it obvious that the calculation of $\langle \mathbf{F}_{\mathrm{sca},i} \rangle$ involves a convolution. In order to make this more clear, the complex 3-vector $\mathbf{F}_{ij}$ in Eq. (20) is expressed in terms of complex 3×3 matrices:

$$\mathbf{F}_{ij} = (\mathbf{p}_{i,0}^{*} \cdot \mathbf{M}_{ij,\gamma} \mathbf{p}_{j,0}) \hat{\mathbf{e}}_{\gamma}. \tag{21}$$

The index γ is over Cartesian coordinates, $\gamma = \{x,y,z\}$, the vectors $\hat{\mathbf{e}}_{\gamma}$ are basis vectors, and the Einstein summation convention over Greek indices is assumed. The complex 3×3 matrices $\mathbf{M}_{ij,\gamma}$ depend only on k and $\mathbf{r}_{ij}$. They are defined as follows:

$$\begin{aligned} \mathbf{M}_{ij,\gamma} = \exp(ikr_{ij}) \Bigg[& (\mathbf{U}_{ij,\gamma} + \mathbf{V}_{ij,\gamma} + \mathbf{W}_{ij,\gamma} - 5\mathbf{T}_{ij,\gamma}) \\ & \times \left(-\frac{k^2}{r_{ij}^2} - \frac{3ik}{r_{ij}^3} + \frac{3}{r_{ij}^4} \right) \\ & + (\mathbf{U}_{ij,\gamma} - \mathbf{T}_{ij,\gamma}) \left(\frac{ik^3}{r_{ij}} - \frac{k^2}{r_{ij}^2} \right) \Bigg], \end{aligned} \tag{22}$$

$$\mathbf{T}_{ij,\gamma} = \hat{n}_{ij,\gamma} (\hat{\mathbf{n}}_{ij} \hat{\mathbf{n}}_{ij}), \qquad \mathbf{U}_{ij,\gamma} = \hat{n}_{ij,\gamma} \mathbf{1},$$

$$\mathbf{V}_{ij,\gamma} = \hat{\mathbf{n}}_{ij} \boldsymbol{\Delta}_{\gamma}, \qquad \mathbf{W}_{ij,\gamma} = \boldsymbol{\Delta}_{\gamma} \hat{\mathbf{n}}_{ij}, \tag{23}$$

where the matrix element $\boldsymbol{\Delta}_{\gamma,\eta}$ is the kronecker delta $\delta_{\gamma\eta}$. The γth column of matrix $\mathbf{V}_{ij,\gamma}$ is $\hat{\mathbf{n}}_{ij}$; its other columns contain zeros. Similarly, the γth row of matrix $\mathbf{W}_{ij,\gamma}$ is $\hat{\mathbf{n}}_{ij}$ and its other rows contain zeros. The matrices $\mathbf{T}_{ij,\gamma}$ and $\mathbf{U}_{ij,\gamma}$ are both symmetrical. Although $\mathbf{V}_{ij,\gamma}$ and $\mathbf{W}_{ij,\gamma}$ are not symmetrical on their own, their sum $\mathbf{V}_{ij,\gamma} + \mathbf{W}_{ij,\gamma}$ is symmetrical. Therefore the matrices $\mathbf{M}_{ij,\gamma}$ are symmetrical. The matrices are antisymmetrical in the pair of indices i and j, since the unit vector $\hat{\mathbf{n}}_{ij}$ appears in odd powers. When we introduce

Table 1. Range of Refractive Indices Used in the Tests, Together with the Number of Dipoles per Wavelength in the DDA Simulations

m	Material	Dipoles per Wavelength
1.05	Biological cells	15
1.14 + 0.38i	H_2O at 10 K for $\lambda = 0.1\ \mu$m	
1.33 + 0.01i	Dirty ice	
1.68 + 0.03i	Amorphous silicate for $\lambda = 1\ \mu$m	20
1.7 + 0.156i		
1.81 + 0.48i	H_2O at 10 K for $\lambda = 0.15\ \mu$m	
2.5 + 1.4i	Graphite	30
3.05 + 0.33i	Amorphous silicate for $\lambda = 90\ \mu$m	40

$$\mathbf{M}_{\gamma} = \begin{bmatrix} 0 & \mathbf{M}_{12,\gamma} & \cdots & \mathbf{M}_{1N,\gamma} \\ \mathbf{M}_{21,\gamma} & \ddots & & \vdots \\ \vdots & & \ddots & \mathbf{M}_{N-1,N,\gamma} \\ \mathbf{M}_{N1,\gamma} & \cdots & \mathbf{M}_{N,N-1,\gamma} & 0 \end{bmatrix} \tag{24}$$

and

$$\mathbf{P} = \begin{pmatrix} \mathbf{p}_{1,0} \\ \vdots \\ \mathbf{p}_{N,0} \end{pmatrix}, \tag{25}$$

$\langle \mathbf{F}_{\mathrm{sca}} \rangle$ can be written as

$$\langle \mathbf{F}_{\mathrm{sca}} \rangle = (\mathbf{P}^{*} \cdot \mathbf{M}_{\gamma} \mathbf{P}) \hat{\mathbf{e}}_{\gamma}. \tag{26}$$

As an intermediate step the scattering force on dipole i can be calculated by

$$\langle \mathbf{F}_{\mathrm{sca},i} \rangle = \mathbf{P}_{i,\eta}^{*} (\mathbf{M}_{\gamma} \mathbf{P})_{3i+\eta} \hat{\mathbf{e}}_{\gamma}, \tag{27}$$

where again the summation convention over greek indices is assumed.

Because the dipoles are arranged in a rectangular grid and their coordinates merely appear in the form $\mathbf{r}_{ij} = \mathbf{r}_i - \mathbf{r}_j$, the matrix vector product $\mathbf{M}_{\gamma}\mathbf{P}$ in Eq. (26) is a discrete convolution, and this product can be evaluated with $O(N \log N)$ complexity by using fast Fourier transforms.

3. TESTS ON SPHERES

As a test case we study the radiation force on a sphere. Using Mie theory and the DDA, we calculate the total radiation force on the sphere. In the case of DDA simulations we calculate $\langle \mathbf{F}_{\mathrm{sca}} \rangle$ directly from the dipole polarizabilities, i.e., from Eq. (26), and also by integration of the scattered field, i.e., by applying Eq. (12). In the latter case a two-dimensional version of the Romberg integration method is applied.[32] For the DDA simulations we apply the previously developed parallel fast DDA method.[33,34] We have carried out a very large number of tests. Here we show a representative subset; details can be found elsewhere.[35]

We performed tests on spheres with three size parameters, $x = 2\pi r/\lambda = 2.5, 5, 10$. Furthermore, we considered a large range of refractive indices, inspired by the typical materials that we wish to study. Table 1 shows the refractive indices that we used, in combination with the size of the dipoles that were used in the DDA simulations. This very important parameter determines the ac-

curacy of the DDA to a large extent. We always take it such that $\lambda/[d\ \mathrm{Re}(m)] \sim 10$ to 15.[33,34,36] Here, m is the relative refractive index and d the diameter of the dipoles (i.e., the grid spacing). The resulting DDA models contain 912 dipoles in the smallest sphere with $m = 1.05$ up to 436,400 for the $x = 10$, $m = 2.5 + 1.4i$ sphere.

Figures 1–3 show the forces on each dipole for the $x = 2.5$ sphere with $m = 1.05$, $1.33 + 0.01i$, and $1.14 + 0.38i$, respectively. In these figures half of the sphere is removed. The incident light travels from right to left and was polarized in the y direction. The first two spheres (Figs. 1 and 2) seem to be pulled in the positive z direction by forces that are largest in the back (left side) of the sphere. In the case of large absorption, as in Fig. 3, the largest forces are in front of the sphere, and it seems to be pushed in the positive z direction. Clearly there is a close connection between the forces on the dipoles and the internal field in the particle. In a previous paper we investigated the internal fields in volume integral equation formalism, a method closely related to the DDA.[36] In that paper we noticed a clear distinction between the internal fields for particles with and without large absorption.

In Tables 2 and 3 we present results of calculations of $\mathbf{g}C_{\mathrm{sca}}$ and of $\mathbf{C}_{\mathrm{pr}}$, which are related to the forces as defined in Subsection 2.A. In Table 2 the results of the z component of $\mathbf{g}C_{\mathrm{sca}}$ and $\mathbf{C}_{\mathrm{pr}}$ are presented. The results from Mie theory, from direct calculations of the forces per dipole and from integration of the scattered field are shown. The incident light was in the positive z direction and polarized in the y direction. In the integration of the scattered fields the Romberg method was always iterated until a precision of at least six digits was obtained.[35] Table 3 shows the results for the x and y components of

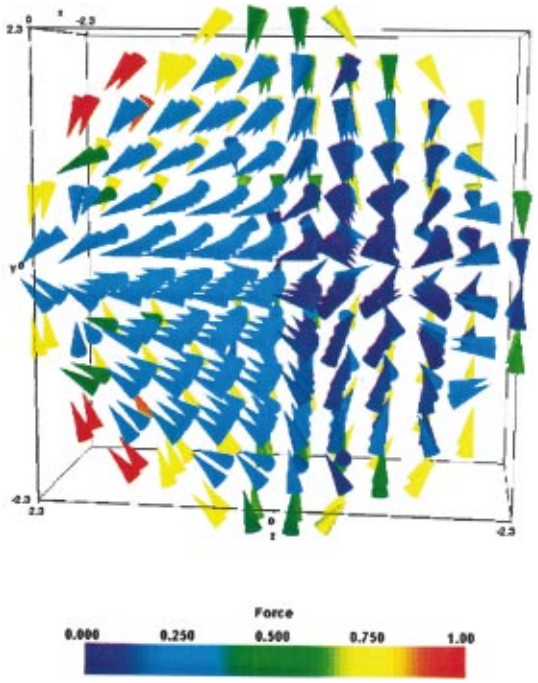

Fig. 1. Total radiation force on each dipole for a sphere with $x = 2.5$ and $m = 1.05$. The incident light travels from right to left. The maximum force is scaled to 1. Only one half of the sphere is shown.

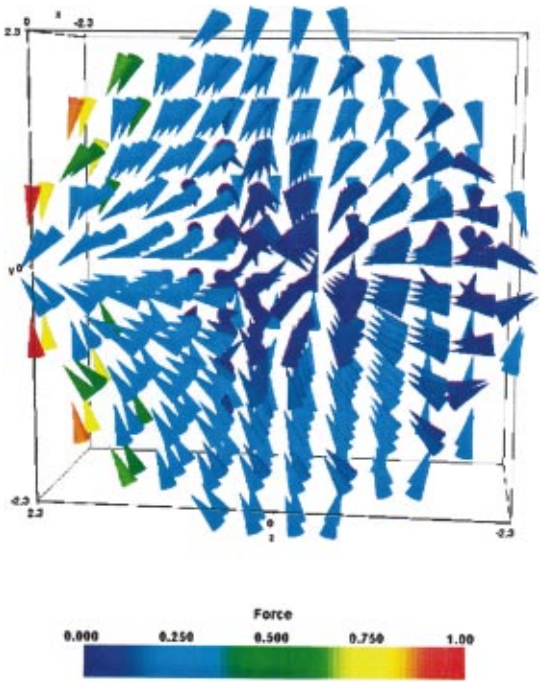

Fig. 2. As Fig. 1 but for $m = 1.33 + 0.01i$.

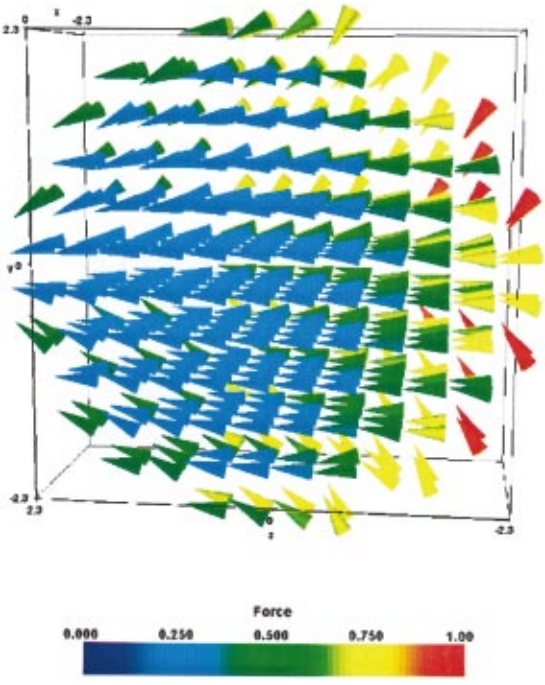

Fig. 3. As Fig. 1 but for $m = 1.14 + 038i$.

$\mathbf{g}C_{\mathrm{sca}}$, which for a sphere must be equal to zero. Finally, in Table 4 we show the relative error between Mie theory and the DDA for C_{ext} and $\mathbf{C}_{\mathrm{pr},z}$ with the latter being obtained by direct calculation of the forces on each dipole.

The first thing to notice from Table 2 is that in all cases that we considered, the direct calculation of the force and subsequent summation leads to the same numerical results as integration of the scattered fields. This was expected on theoretical grounds as presented in Subsection

2.A, but the results in Table 2 show that our numerical procedures do not induce extra errors.

For a sphere with incident radiation in the z direction, the x and y components of the radiation force are exactly zero. Table 3 shows that the direct calculation of the forces indeed results in very small x and y components. The direct method results in almost all cases in x and y components on the order of 10^{-6} to 10^{-8} times the z component. This very small remaining fraction is attributed to round-off errors in the numerical calculations. The integration of the scattered fields show somewhat different results. The y component is also very small, comparable with that of the direct method. However, for the x component (i.e., perpendicular to the polarization of the incident field) the integration results in small (as compared with the z component) but finite values of $\mathbf{g}_x C_{\mathrm{sca}}$. In-

Table 2. Results of Calculations of $\mathbf{g}_z C_{\mathrm{sca}}$ and $\mathbf{C}_{\mathrm{pr},z}$ for Spheres As a Function of the Size Parameter x and Relative Refractive Index m[a]

		$\mathbf{g}_z C_{\mathrm{sca}}$			$\mathbf{C}_{\mathrm{pr},z}$		
x	m	Mie	Direct	Integration	Mie	Direct	Integration
2.51994	1.05	0.371524	0.371659	0.371666	0.122651	0.122112	0.122112
2.51994	1.14 + 0.38i	8.24625	8.27892	8.27892	26.9337	26.9879	26.9879
2.51994	1.33 + 0.01i	16.7049	16.6745	16.6745	8.64969	8.53591	8.53591
2.52546	1.68 + 0.03i	52.2132	53.1363	53.1363	30.6572	30.0432	30.0432
2.52546	1.70 + 0.156i	33.7644	35.0417	35.0417	35.8229	35.8576	35.8576
2.52546	1.81 + 0.48i	20.9415	21.8652	21.8652	38.6260	39.3070	39.3070
2.50977	2.50 + 1.40i	18.9673	20.1332	20.1332	38.4895	39.8698	39.8698
2.51808	3.05 + 0.33i	21.3637	23.0295	23.0296	37.6059	38.3417	38.3417
5.01954	1.05	8.57554	8.57815	8.57815	0.859150	0.863781	0.863790
5.01954	1.14 + 0.38i	63.8590	63.7802	63.7802	105.156	105.065	105.065
5.01954	1.33 + 0.01i	222.436	223.542	223.542	53.823	53.4137	53.4137
5.03617	1.68 + 0.03i	60.2681	62.5525	62.5525	112.658	111.251	111.251
5.03617	1.70 + 0.156i	73.1439	73.6662	73.6662	127.300	127.694	127.694
5.03617	1.81 + 0.48i	83.2464	84.2083	84.2083	123.102	124.179	124.179
5.02511	2.50 + 1.40i	87.541	88.8857	88.8856	121.662	123.694	123.694
10.0502	1.05	150.276	150.258	150.258	4.65605	4.66638	4.66626
10.0502	1.14 + 0.38i	315.490	315.302	315.302	384.379	384.237	384.236
10.0502	1.33 + 0.01i	438.904	441.835	441.835	262.641	263.107	263.106

[a] Calculations were performed with Mie theory and the DDA. In the latter the forces on the dipoles were calculated, and subsequently $\mathbf{g}_z C_{\mathrm{sca}}$ and $\mathbf{C}_{\mathrm{pr},z}$ were obtained (column "Direct"). Also from the DDA the scattered field was calculated, and $\mathbf{g}_z C_{\mathrm{sca}}$ and $\mathbf{C}_{\mathrm{pr},z}$ were obtained by an integration of the scattered field (column "Integration").

Table 3. As in Table 2, but with the x and y Component of $\mathbf{g}C_{\mathrm{sca}}$[a]

		$\mathbf{g}_x C_{\mathrm{sca}}$		$\mathbf{g}_y C_{\mathrm{sca}}$	
x	m	Direct	Integration	Direct	Integration
2.51994	1.05	3.1×10^{-9}	0.0018	1.7×10^{-9}	1.6×10^{-9}
2.51994	1.14 + 0.38i	-2.1×10^{-9}	0.036	8.6×10^{-8}	2.9×10^{-8}
2.51994	1.33 + 0.01i	6.3×10^{-7}	0.071	-1.9×10^{-7}	2.7×10^{-7}
2.52546	1.68 + 0.03i	1.8×10^{-6}	0.18	1.4×10^{-6}	2.4×10^{-6}
2.52546	1.70 + 0.156i	9.3×10^{-7}	0.12	-2.6×10^{-7}	1.8×10^{-6}
2.52546	1.81 + 0.48i	1.0×10^{-6}	0.079	1.9×10^{-6}	8.3×10^{-7}
2.50977	2.50 + 1.40i	-1.3×10^{-6}	0.092	2.4×10^{-6}	8.6×10^{-7}
2.51808	3.05 + 0.33i	3.9×10^{-6}	0.095	-3.5×10^{-6}	3.1×10^{-7}
5.01954	1.05	6.5×10^{-8}	0.017	3.7×10^{-8}	2.0×10^{-8}
5.01954	1.14 + 0.38i	3.2×10^{-8}	0.14	1.6×10^{-6}	1.2×10^{-6}
5.01954	1.33 + 0.01i	1.6×10^{-5}	0.45	9.8×10^{-6}	1.0×10^{-5}
5.03617	1.68 + 0.03i	4.9×10^{-6}	0.30	8.0×10^{-6}	1.1×10^{-5}
5.03617	1.70 + 0.156i	3.7×10^{-7}	0.17	2.7×10^{-6}	1.4×10^{-6}
5.03617	1.81 + 0.48i	6.1×10^{-7}	0.20	6.7×10^{-7}	-1.8×10^{-7}
5.02511	2.50 + 1.40i	-4.7×10^{-6}	0.29	-1.1×10^{-5}	-1.9×10^{7}
10.0502	1.05	1.2×10^{-6}	0.15	6.1×10^{-7}	7.1×10^{-7}
10.0502	1.14 + 0.38i	-4.6×10^{-6}	0.43	3.5×10^{-6}	-3.4×10^{-6}
10.0502	1.33 + 0.01i	1.0×10^{-4}	1.1	9.1×10^{-5}	7.8×10^{-5}

[a] Only the DDA results are shown. The exact result is zero in all cases.

Table 4. Relative Error in C_{ext} and $C_{pr,z}$ in DDA Simulations of Spheres[a]

x	m	Error in C_{ext} (percent)	Error in $C_{pr,z}$ (percent)
2.51994	1.05	0.08	0.44
2.51994	1.14 + 0.38i	0.25	0.20
2.51994	1.33 + 0.01i	0.57	1.32
2.52546	1.68 + 0.03i	0.37	2.00
2.52546	1.70 + 0.156i	1.89	0.10
2.52546	1.81 + 0.48i	2.69	1.76
2.50977	2.50 + 1.40i	4.43	3.59
2.51808	3.05 + 0.33i	4.07	1.96
5.01954	1.05	0.08	0.54
5.01954	1.14 + 0.38i	0.10	0.09
5.01954	1.33 + 0.01i	0.25	0.76
5.03617	1.68 + 0.03i	0.51	1.25
5.03617	1.70 + 0.156i	0.46	0.31
5.03617	1.81 + 0.48i	0.99	0.87
5.02511	2.50 + 1.40i	1.61	1.67
10.0502	1.05	0.00	0.22
10.0502	1.14 + 0.38i	0.05	0.04
10.0502	1.33 + 0.01i	0.48	0.18

[a] $\mathbf{C}_{pr,z}$ was obtained from a direct calculation of the forces on the dipoles.

creasing the accuracy of the Romberg integration did not remove these finite values. This is probably due to very small errors in the scattered field as calculated by the DDA.

Finally, from Table 4 we can conclude that in all cases considered, the relative error in the radiation pressure coefficient as obtained with the DDA is comparable (i.e., of the same order) with the relative error in the extinction coefficient. Note from Tables 2–4 that we get accurate results, even for very large refractive indices. This is made possible by carefully reducing the size of the dipoles in the DDA model as the refractive index increases (see Table 1). However, as was already noted by other authors,[27–29] it is also clear that even when the dipoles are reduced in size, the accuracy of the DDA results decreases with larger refractive indices.

4. DISCUSSION AND CONCLUSIONS

We presented theoretical expressions to calculate efficiently the radiation force on each dipole in the DDA. This allows us not only to calculate radiation pressure on arbitrarily shaped particles, such as biological particles or dust particles, but also to calculate the radiation forces inside arbitrarily shaped particles. We introduced expressions that allow the calculation of these forces in an $O(N \log N)$ operation count. Finally, we showed theoretically that integrating the scattered fields and summating the forces on each dipole are equivalent. We presented numerical tests on spheres and showed that direct calculation of the dipole forces and integration of the scattered field indeed yield the same results for the radiation-pressure coefficients. Furthermore, we showed that the resulting relative errors in the radiation-pressure coefficients as obtained by the DDA have the same order of magnitude, i.e., on the order of 1%, as the relative error in the extinction coefficient. We did not test the accuracy of the individual force vector on each dipole. However, because the forces are closely connected to the internal fields, we expect behavior comparable with that for the errors in the internal fields.[36] This is still a topic of research.

In principle, the DDA method is also capable of handling other incident beams (e.g., focused laser beams).[37] Therefore it should also be possible to calculate radiation forces on particles in optical traps or optical tweezers. The theory as presented in this paper is still valid for such more complicated incident beams. The expressions for $\langle \mathbf{F}_{sca,i} \rangle$ [Eqs. (19) and (20)] remain valid. Only the expressions for $\langle \mathbf{F}_{inc,i} \rangle$ need to be adapted for a more complicated incident beam.

We will apply our method to calculate radiation forces on grains that make up circumstellar dust particles. We start with aggregates that are generated by using the methods of Dominik and Tielens.[20] We plan to assess the accuracy of the obtained radiation pressure by comparing the results with other methods (e.g., by using the theory of scattering from aggregates of spheres). Next the radiation forces on each grain in the aggregate will be calculated and compared with the other (i.e., the mechanical) forces that play a role in the coagulation. In this way we hope to find out to what extent the radiation forces can influence coagulation of circumstellar dust particles.

APPENDIX A

Calculating $(\mathbf{p}_i^* \cdot \nabla_i)\mathbf{E}_{ij}$ means performing differentiations of the form

$$(\mathbf{p}_{i,0}^* \cdot \nabla_i) f(r_{ij}) = (\mathbf{p}_{i,0}^* \cdot \nabla_i r_{ij}) f'(r_{ij}) = (\mathbf{p}_{i,0}^* \cdot \hat{\mathbf{n}}_{ij}) f'(r_{ij}), \tag{A1}$$

where the functions f are combinations of $1/r^\alpha$, with α an integer, or the complex exponential. The differentiation of the vector function can be rewritten as

$$(\mathbf{p}_{i,0}^* \cdot \nabla_i)\hat{\mathbf{n}}_{ij}(\hat{\mathbf{n}}_{ij} \cdot \mathbf{p}_{j,0}) = \frac{1}{r_{ij}}[(\mathbf{p}_{i,0}^* \cdot \mathbf{p}_{j,0})\hat{\mathbf{n}}_{ij} + \mathbf{p}_{i,0}^*(\hat{\mathbf{n}}_{ij} \cdot \mathbf{p}_{j,0}) - 2(\mathbf{p}_{i,0}^* \cdot \hat{\mathbf{n}}_{ij})\hat{\mathbf{n}}_{ij}(\hat{\mathbf{n}}_{ij} \cdot \mathbf{p}_{j,0})]. \tag{A2}$$

Carrying out all the algebra and using Eqs. (A1) and (A2) finally results in

$$(\mathbf{p}^*_{i,0}\cdot\nabla_i)\mathbf{E}_{ij} = \exp(ikr_{ij})\Bigg\{(\mathbf{p}^*_{i,0}\cdot\mathbf{p}_{j,0})\hat{\mathbf{n}}_{ij}\times\left(-\frac{k^2}{r_{ij}^2}-\frac{3ik}{r_{ij}^3}+\frac{3}{r_{ij}^4}\right)-(\mathbf{p}^*_{i,0}\cdot\hat{\mathbf{n}}_{ij})\hat{\mathbf{n}}_{ij}(\hat{\mathbf{n}}_{ij}\cdot\mathbf{p}_{j,0})\times\left[5\left(-\frac{k^2}{r_{ij}^2}-\frac{3ik}{r_{ij}^3}+\frac{3}{r_{ij}^4}\right)+\frac{ik^3}{r_{ij}}-\frac{k^2}{r_{ij}^2}\right]+(\mathbf{p}^*_{i,0}\cdot\hat{\mathbf{n}}_{ij})\mathbf{p}_{j,0}\times\left(\frac{ik^3}{r_{ij}}-\frac{2k^2}{r_{ij}^2}-\frac{3ik}{r_{ij}^3}+\frac{3}{r_{ij}^4}\right)+\mathbf{p}^*_{i,0}(\hat{\mathbf{n}}_{ij}\cdot\mathbf{p}_{j,0})\left(-\frac{k^2}{r_{ij}^2}-\frac{3ik}{r_{ij}^3}+\frac{3}{r_{ij}^4}\right)\Bigg\}. \tag{A3}$$

APPENDIX B

In this section the integral in Eq. (12) will be solved analytically. The final expression, as expected, is equal to $-\langle\mathbf{F}_{\mathrm{sca}}\rangle$. First, Eq. (12) is cast into a different form,

$$\langle\mathbf{F}_{\mathrm{out}}\rangle = \frac{k^4}{8\pi}\sum_{i,j}^{N}\int \mathrm{d}\Omega\hat{\mathbf{n}}I_{ij}(\hat{\mathbf{n}}) = \sum_{i,j}^{N}\langle\mathbf{F}_{I,ij}\rangle, \tag{B1}$$

with

$$I_{ij}(\hat{\mathbf{n}}) = \exp(ik\hat{\mathbf{n}}\cdot\mathbf{r}_{ij})[\mathbf{p}^*_{i,0}\cdot\mathbf{p}_{j,0}-(\mathbf{p}^*_{i,0}\cdot\hat{\mathbf{n}})(\hat{\mathbf{n}}\cdot\mathbf{p}_{j,0})]. \tag{B2}$$

The reversal of summation and integration is of no concern, since the number of dipoles N is large but finite. The relation

$$\left|\sum_{i=1}^{N}[\mathbf{p}_{i,0}-\hat{\mathbf{n}}(\hat{\mathbf{n}}\cdot\mathbf{p}_{i,0})]\exp(-ik\hat{\mathbf{n}}\cdot\mathbf{r}_i)\right|^2 = \sum_{i,j}^{N}I_{ij}(\hat{\mathbf{n}})$$

follows easily from working out the left-hand side. Furthermore, one should notice that $I_{ij}(\hat{\mathbf{n}}) = I^*_{ji}(\hat{\mathbf{n}})$, which causes the imaginary parts of each integral term ij and ji in the double summation to cancel. The actual evaluation of the integration in Eq. (B1) is complicated by the exponential factor

$$\exp(-ik\hat{\mathbf{n}}\cdot\mathbf{r}_{ij}) = \exp[ik(r_{ij,x}\sin\theta\cos\phi + r_{ij,y}\sin\theta\sin\phi + r_{ij,z}\cos\theta)],$$

which arises for factors $i\neq j$; θ and ϕ are the usual polar angles. Considering each integral term separately and aligning the z axis for the spherical coordinates parallel to r_{ij} can reduce the complexity of the integrals considerably. In this case the complex exponent is $ikr_{ij}\cos\theta$. Working out in Eq. (B1) full detail will show that it is possible to separate each term into a θ- and a ϕ-dependent part. The integration of the ϕ-dependent parts is straightforward; the θ-dependent parts need some more attention. All θ-dependent integrals are of the form

$$\Theta = \int_0^{\pi}\sin(\theta)f(\cos\theta)\exp(ikr_{ij}\cos\theta)\mathrm{d}\theta, \tag{B3}$$

where f is a polynomial function of $\cos\theta$. This is justified, because working out Eq. (B1) will show that only those ϕ-dependent parts that do not vanish have corresponding θ-dependent parts with only even powers of $\sin\theta$. So there is no case where f contains odd powers of $(1-\cos^2\theta)^{1/2}$ but only even powers. Therefore f will merely be a polynomial in $\cos\theta$. Substituting $t=\cos\theta$ reduces Eq. (B3) to

$$\Theta = \int_{-1}^{1}f(t)\exp(ikr_{ij}t)\mathrm{d}t.$$

The integral

$$I_u(\alpha) = \int_{-1}^{1}t^u\exp(ik\alpha t)\mathrm{d}t \tag{B4}$$

will be solved in Appendix C. With all expressions at hand, writing down the solutions to Eq. (B1) is a matter of accurate administration. For the details we refer to Appendix D. Introducing the variables

$$a_{ij} = \exp(ikr_{ij}),\qquad b_{1,ij} = -\frac{k^2}{r_{ij}^2}-\frac{3ik}{r_{ij}^3}+\frac{3}{r_{ij}^4},$$

$$b_{2,ij} = \frac{ik^3}{r_{ij}}-\frac{k^2}{r_{ij}^2},$$

$$\mathbf{c}_{1,ij} = \begin{pmatrix}\mathbf{p}^*_{i,0,x}\mathbf{p}_{j,0,z}+\mathbf{p}^*_{i,0,z}\mathbf{p}_{j,0,x}\\ \mathbf{p}^*_{i,0,y}\mathbf{p}_{j,0,z}+\mathbf{p}^*_{i,0,z}\mathbf{p}_{j,0,y}\\ \mathbf{p}^*_{i,0,x}\mathbf{p}_{j,0,x}+\mathbf{p}^*_{i,0,y}\mathbf{p}_{j,0,y}-2\mathbf{p}^*_{i,0,z}\mathbf{p}_{j,0,z}\end{pmatrix},$$

$$\mathbf{c}_{2,ij} = (\mathbf{p}^*_{i,0,x}\mathbf{p}_{j,0,x}+\mathbf{p}^*_{i,0,y}\mathbf{p}_{j,0,y})\hat{\mathbf{e}}_z,$$

the integrated scattering force becomes

$$-\langle\mathbf{F}_{I,ij}\rangle = \frac{1}{2}[\mathrm{Im}(a_{ij}b_{1,ij})\mathrm{Im}(\mathbf{c}_{1,ij})+\mathrm{Im}(a_{ij}b_{2,ij})\mathrm{Im}(\mathbf{c}_{2,ij})]. \tag{B5}$$

Let us now investigate how this compares with the expressions for $\langle\mathbf{F}_{\mathrm{sca}}\rangle$ as derived in Section 2. After inserting $\hat{\mathbf{n}}_{ij}=\hat{\mathbf{e}}_z$ into $\mathbf{F}_{ij}$ in Eq. (20) and using the same dummy variables, we find that

$$\begin{aligned}\tfrac{1}{2}\mathrm{Re}(\mathbf{F}_{ij}) &= \tfrac{1}{2}\mathrm{Re}(a_{ij}b_{1,ij}\mathbf{c}_{1,ij}+a_{ij}b_{2,ij}\mathbf{c}_{2,ij})\\ &= \tfrac{1}{2}\mathrm{Re}[\mathrm{Re}(a_{ij}b_{1,ij})\mathrm{Re}(\mathbf{c}_{1,ij})-\mathrm{Im}(a_{ij}b_{1,ij})\mathrm{Im}(\mathbf{c}_{1,ij})+\mathrm{Re}(a_{ij}b_{2,ij})\times\mathrm{Re}(\mathbf{c}_{2,ij})-\mathrm{Im}(a_{ij}b_{2,ij})\mathrm{Im}(\mathbf{c}_{2,ij})].\end{aligned} \tag{B6}$$

Clearly,

$$-\langle\mathbf{F}_{I,ij}\rangle \neq \tfrac{1}{2}\mathrm{Re}(\mathbf{F}_{ij}),$$

but

$$-\langle\mathbf{F}_{I,ij}\rangle-\langle\mathbf{F}_{I,ji}\rangle = \tfrac{1}{2}\mathrm{Re}(\mathbf{F}_{ij})+\tfrac{1}{2}\mathrm{Re}(\mathbf{F}_{ji}). \tag{B7}$$

This is true because $\mathbf{c}_{1,ij}=-\mathbf{c}^*_{1,ji}$ and $\mathbf{c}_{2,ij}=-\mathbf{c}^*_{2,ji}$. Therefore the scattering force $\langle\mathbf{F}_{\mathrm{sca}}\rangle$ as obtained from summation of forces on each dipole, i.e., Eqs. (5), (19), and (20), is exactly equal to $-\langle\mathbf{F}_{\mathrm{out}}\rangle$. The result of numerical integration will therefore converge to that of direct calculation of the forces from the dipole polarizabilities.

Note that the same reasoning can be applied to the scattering cross section C_{sca}. In the DDA it can be directly calculated from the difference between the extinction cross section and the absorption cross section, for which exact formulas are available.[27] It can also be calculated by integrating the far-field scattered intensity, i.e., by removing the factor $\hat{\mathbf{n}}$ in the integrand of Eq. (12). This integral can be solved analytically in the same way as we did for the scattering force and is equal to the exact result obtained from the extinction cross section and the absorption cross section.

APPENDIX C

The evalution of $I_u(\alpha)$ comes down to multiple partial integration. We use the following recursion relation between $I_u(\alpha)$ and $I_{u-1}(\alpha)$,

$$I_u(\alpha) = \int_{-1}^{1} t^u \exp(i\alpha t)\mathrm{d}t = \frac{\exp(i\alpha) + \exp(-i\alpha)(-1)^{u+1}}{i\alpha} - \frac{uI_{u-1}(\alpha)}{i\alpha}, \tag{C1}$$

valid for $u \geqslant 1$ and $\alpha \neq 0$. We explicitly expand $I_u(\alpha)$ for $u \leqslant 3$:

$$\begin{aligned}
I_0(\alpha) &= [\exp(i\alpha) - \exp(-i\alpha)]\frac{1}{i\alpha},\\
I_1(\alpha) &= [\exp(i\alpha) + \exp(-i\alpha)]\frac{1}{i\alpha} - [\exp(i\alpha) - \exp(-i\alpha)]\frac{1}{(i\alpha)^2},\\
I_2(\alpha) &= [\exp(i\alpha) - \exp(-i\alpha)]\left[\frac{1}{i\alpha} + \frac{2}{(i\alpha)^3}\right] - [\exp(i\alpha) + \exp(-i\alpha)]\frac{2}{(i\alpha)^2},\\
I_3(\alpha) &= [\exp(i\alpha) + \exp(-i\alpha)]\left[\frac{1}{i\alpha} + \frac{6}{(i\alpha)^3}\right] - [\exp(i\alpha) - \exp(-i\alpha)] \times \left[\frac{3}{(i\alpha)^2} + \frac{6}{(i\alpha)^4}\right].
\end{aligned} \tag{C2}$$

For further use some combinations are calculated and cast into a different form:

$$I_1(\alpha) = 2i\,\mathrm{Im}\left[\exp(i\alpha)\left\{-\frac{i}{\alpha} + \frac{1}{\alpha^2}\right\}\right],$$

$$I_3(\alpha) - I_1(\alpha) = 4i\,\mathrm{Im}\left[\exp(i\alpha)\left\{\frac{1}{\alpha^2} + \frac{3i}{\alpha^3} - \frac{3}{\alpha^4}\right\}\right]. \tag{C3}$$

APPENDIX D

Before the integral is solved, we introduce the dyadic

$$\mathbf{N}(t,\phi) = \hat{\mathbf{n}}\hat{\mathbf{n}} = \begin{bmatrix} \cos^2(\phi)s^2(t) & \cos(\phi)\sin(\phi)s^2(t) & \cos(\phi)ts(t) \\ \cos(\phi)\sin(\phi)s^2(t) & \sin^2(\phi)s^2(t) & \sin(\phi)ts(t) \\ \cos(\phi)ts(t) & \sin(\phi)ts(t) & t^2 \end{bmatrix}, \tag{D1}$$

with $s(t) = \sqrt{1-t^2}$. The integral terms in Eq. (B1) become

$$\langle \mathbf{F}_{I,ij} \rangle = \frac{k^4}{8\pi}\int_0^{2\pi}\mathrm{d}\phi\int_{-1}^{1}\mathrm{d}\mathbf{t}\exp(ikr_{ij}t) \times \begin{pmatrix} s(t)\cos(\phi) \\ s(t)\sin(\phi) \\ t \end{pmatrix}[(\mathbf{p}^*_{i,0}\cdot\mathbf{p}_{j,0}) - \mathbf{p}^*_{i,0}\cdot\mathbf{N}(t,\phi)\mathbf{p}_{j,0}]. \tag{D2}$$

In the first term of the integrand only the z component does not vanish. The second term consists of 27 integrals, a sum of 9 for each spatial direction. Piecewise evaluation of the ϕ-dependent parts shows that only 7 of those integrals do not vanish. These integrals are as follows: in the x direction the terms corresponding to $\mathbf{N}_{13}$ and $\mathbf{N}_{31}$, in the y direction the terms corresponding to $\mathbf{N}_{23}$ and $\mathbf{N}_{32}$, and in the z direction the terms corresponding to the diagonal elements of $\mathbf{N}$. This reduces Eq. (D2) to

$$\langle \mathbf{F}_{I,ij} \rangle = \frac{k^4[I_3(kr_{ij}) - I_1(kr_{ij})]}{8} \times \begin{pmatrix} \mathbf{p}^*_{i,0,x}\cdot\mathbf{p}_{j,0,z} + \mathbf{p}^*_{i,0,z}\cdot\mathbf{p}_{j,0,x} \\ \mathbf{p}^*_{i,0,y}\cdot\mathbf{p}_{j,0,z} + \mathbf{p}^*_{i,0,z}\cdot\mathbf{p}_{j,0,y} \\ \mathbf{p}^*_{i,0,x}\cdot\mathbf{p}_{j,0,x} + \mathbf{p}^*_{i,0,y}\cdot\mathbf{p}_{j,0,y} - 2\mathbf{p}^*_{i,0,z}\cdot\mathbf{p}_{j,0,z} \end{pmatrix} + \frac{k^4 I_1(kr_{ij})}{4}\begin{pmatrix} 0 \\ 0 \\ \mathbf{p}^*_{i,0,x}\cdot\mathbf{p}_{j,0,x} + \mathbf{p}^*_{i,0,y}\cdot\mathbf{p}_{j,0,y} \end{pmatrix}. \tag{D3}$$

For $i = j$ the argument α in Eq. (C1) is zero. In that case $I_u(0) = 0$ if u is an odd number. From Eq. (D3) we immediately see that in that case the integral is zero.

ACKNOWLEDGMENTS

We thank R. Belleman and D. Hannema, both of the University of Amsterdam, for their help in creating Figs. 1–3. L. B. F. M. Waters acknowledges financial support from the Dutch Science Foundation NWO, Pioneer grant 616.078.333.

A. G. Hoekstra, M. Frijlink, and P. M. A. Sloot can be reached at their address on the title page; phone, 31-20-

5257463; fax, 31-20-5257490. A. G. Hoekstra's e-mail address is alfons@science.uva.nl. http://www.science.uva.nl/research/scs.

REFERENCES

1. P. Debye, "Der Lichtdruck auf Kugeln von beliebigem Material," Ann. Phys. (Leipzig) **30**, 57–136 (1909).
2. C. F. Bohren and D. R. Huffman, *Absorption and Scattering of Light by Small Particles* (Wiley, New York, 1983).
3. A. Ashkin, "Acceleration and trapping of particles by radiation pressure," Phys. Rev. Lett. **24**, 156–159 (1970).
4. A. Ashkin and J. M. Dziedzic, "Optical levitation by radiation pressure," Appl. Phys. Lett. **19**, 283–285 (1971).
5. A. Ashkin and J. M. Dziedzic, "Observation of light scattering from nonspherical particles using optical levitation," Appl. Opt. **19**, 660–668 (1980).
6. A. Ashkin and J. M. Dziedzic, "Optical trapping and manipulation of viruses and bacteria," Science **235**, 1517–1520 (1987).
7. S. Chu, "The manipulation of neutral particles," Rev. Mod. Phys. **60**, 685–706 (1998).
8. K. Visscher, G. J. Brakenhoff, and J. J. Krol, "Micromanipulation by "multiple" optical traps created by a single fast scanning trap integrated with the bilateral confocal scanning laser microscope," Cytometry **14**, 105–114 (1993).
9. K. O. Greulich, *Micromanipulation by Light in Biology and Medicine: The Laser Microbeam and Optical Tweezers* (Birkhauser, Boston, Mass., 1999).
10. P. J. H. Bronkhorst, G. J. Streekstra, J. Grimbergen, E. J. Nijhof, J. J. Sixma, and G. J. Brakenhoff, "A new method to study shape recovery of red blood cells using multiple optical trapping," Biophys. J. **69**, 1666–1673 (1995).
11. S. B. Smith, Y. Cui, and C. Bustamante, "Overstretching B-DNA: the elastic response of individual double-stranded and single-stranded DNA molecules," Science **271**, 795–799 (1996).
12. T. R. Lettieri, W. D. Jenkins, and D. A. Swyt, "Sizing of individual optically levitated evaporating droplets by measurement of resonances in the polarization ratio," Appl. Opt. **20**, 2799–2805 (1981).
13. F. Guilloteau, G. Grehan, and G. Gousbet, "Optical levitation experiments to assess the validity of the generalized Lorenz–Mie theory," Appl. Opt. **31**, 2942–2951 (1992).
14. R. M. P. Doornbos, M. Schaeffer, A. G. Hoekstra, P. M. A. Sloot, B. G. de Grooth, and J. Greve, "Elastic light scattering measurements of single biological cells in an optical trap," Appl. Opt. **34**, 729–734 (1996).
15. B. T. Draine and J. C. Weingartner, "Radiative torques on interstellar grains I. Superthermal spin-up," Astrophys. J. **470**, 551–565 (1996).
16. B. T. Draine and J. C. Weingartner, "Radiative torques on interstellar grains II. Grain alignment," Astrophys. J. **480**, 633–646 (1997).
17. A. Kriviv, H. Kimura, and I. Mann, "Dynamics of dust near the sun," Icarus **134**, 311–327 (1998).
18. H. Kimura and I. Mann, "Radiation pressure cross section for fluffy aggregates," J. Quant. Spectrosc. Radiat. Transf. **60**, 425–438 (1998).
19. T. Mukai, H. Ishimoto, T. Kozasca, J. Blum, and J. M. Greenberg, "Radiation pressure forces of fluffy porous grains," Astron. Astrophys. **262**, 315–320 (1992).
20. C. Dominik and A. G. G. M. Tielens, "The physics of dust coagulation and the structure of dust aggregates in space," Astrophys. J. **480**, 647–673 (1997).
21. C. Dominik and R. Waters, University of Amsterdam, Kruislaan 403, 1098 SJ Amsterdam, The Netherlands (personal communication, 1999).
22. M. I. Mishchenko, J. W. Hovenier, and L. D. Travis, eds., *Light Scattering by Nonspherical Particles* (Academic, San Diego, Calif., 1999).
23. K. Lumme and J. Rahola, "Light scattering by porous dust particles in the discrete-dipole approximation," Astrophys. J. **425**, 653–667 (1994).
24. Z. Xing and M. S. Hanner, "Light scattering by aggregate particles," Astron. Astrophys. **324**, 805–820 (1997).
25. T. Kozasa, J. Blum, and T. Mukai, "Optical properties of dust aggregates I. Wavelength dependence," Astron. Astrophys. **263**, 423–432 (1992).
26. T. Kozasa, J. Blum, H. Okamoto, and T. Mukai, "Optical properties of dust aggregates II. Angular dependence of scattered light," Astron. Astrophys. **276**, 278–288 (1993).
27. B. T. Draine, "The discrete-dipole approximation and its application to interstellar graphite grains," Astrophys. J. **333**, 848–872 (1988).
28. B. T. Draine and P. J. Flatau, "Discrete-dipole approximation for scattering calculations," J. Opt. Soc. Am. A **11**, 1491–1499 (1994).
29. B. T. Draine, "The discrete dipole approximation for light scattering by irregular targets," in *Light Scattering by Nonspherical Particles*, M. I. Mishchenko, J. W. Hovenier, and L. D. Travis, eds. (Academic, San Diego, Calif., 1999), Chap. 5.
30. J. P. Gordon, "Radiation force and momenta in dielectric media," Phys. Rev. A **8**, 14–21 (1973).
31. J. J. Goodman, B. T. Draine, and P. J. Flatau, "Application of fast-Fourier-transform techniques to the discrete-dipole approximation," Opt. Lett. **16**, 1198–2000 (1991).
32. W. H. Press, B. P. Flannery, S. A. Teukolsky, and W. T. Vetterling, *Numerical Recipes in C* (Cambridge U. Press, Cambridge, UK, 1988).
33. A. G. Hoekstra and P. M. A. Sloot, "Coupled dipole simulations of elastic light scattering on parallel systems," Int. J. Mod. Phys. C **6**, 663–679 (1995).
34. A. G. Hoekstra, M. D. Grimminck, and P. M. A. Sloot, "Large scale simulations of elastic light scattering by a fast discrete dipole approximation," Int. J. Mod. Phys. C **9**, 87–102 (1998).
35. M. Frijlink, "Application of the discrete dipole approximation to radiation pressure calculations on dust-aggregates: an exploration," M.Sc. thesis (University of Amsterdam, Amsterdam, 2000).
36. A. G. Hoekstra, J. Rahola, and P. M. A. Sloot, "Accuracy of internal fields in volume integral equation simulations of light scattering," Appl. Opt. **37**, 8482–8497 (1998).
37. A. G. Hoekstra, "Computer simulations of elastic light scattering, implementations and applications," Ph.D. dissertation (University of Amsterdam, Amsterdam, 1994).